JOURNAL OF CHEMICAL INFORMATION AND MODELING

Article

pubs.acs.org/jcim

# Consensus Scoring Approach To Identify the Inhibitors of AMP-Activated Protein Kinase α2 with Virtual Screening

Hwangseo Park,*[,†] Jae-Won Eom,[‡] and Yang-Hee Kim*[,‡]

[†]Department of Bioscience and Biotechnology and [‡]Department of Molecular Biology, Sejong University, 209 Neungdong-ro, Kwangjin-gu, Seoul 143-747, Korea

**ABSTRACT:** Due to the involvement in the ischemic damage in the brain, 5′-adenosine monophosphate-activated protein kinase subunit α2 (AMPK2) serves as a promising target for the development of new medicines for stroke. Despite such a pharmaceutical importance, only a few small-molecule inhibitors have been reported so far. We aim in this study to identify a new class of AMPK2 inhibitors based on the structure-based virtual screening with docking simulations. To take advantage of and supplement the deficiencies of force field-based and empirical scoring functions, a consensus scoring method is employed to select the putative inhibitors by the combined use of AutoDock and FlexX programs. Prior to the virtual screening with docking simulations, both scoring functions are modified by implementing the molecular solvation free energy term to enhance the accuracy in estimating the protein−ligand binding affinity. As a consequence of the consensus virtual screening with the two modified scoring functions, we find seven structurally diverse AMPK2 inhibitors with micromolar inhibitory activity. Detailed binding mode analyses indicate that all these inhibitors can be stabilized in the ATP-binding pocket through the simultaneous establishment of the multiple hydrogen bonds and hydrophobic interactions. It is also found that a high inhibitory activity can be achieved by the reduction of desolvation cost for the inhibitor as well as by the strengthening of the enzyme−inhibitor interactions. Thus, the results of the present study demonstrate the outperformance of consensus scoring with the force field-based and empirical scoring functions that are modified to include the effects of ligand solvation on protein−ligand docking.

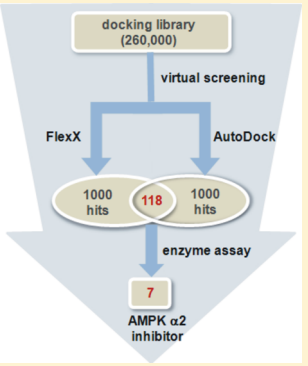


## INTRODUCTION

5′-Adenosine monophosphate-activated protein kinase (AMPK) is a member of the serine/threonine kinase subfamily and serves as an energy sensor that monitors the cellular energy status and thereby regulates the metabolism at the whole-body level.[1] Besides the role of maintaining energy homeostasis, AMPK has also been appreciated to be involved in the neuronal response to stress. Related with the activity for neuronal metabolism, the overactivation of AMPK has a deleterious effect on the central nervous system and can be responsible for the pathogenesis of ischemic stroke.[2] AMPK acts in the form of a heterotrimeric enzyme complex in which the catalytic α subunit including a kinase domain is stabilized by the intermolecular interactions with the regulatory β and γ subunits. Two isoforms exist for the α subunit, α1 and α2, which have a functional redundancy in food intake and energy expenditure.[3] Although both α1 and α2 are responsible for the ischemic damage in the brain, a significant neuroprotective effect was observed only in the absence of the activity of α2 subunit of AMPK (AMPK2).[4,5] Therefore, the impairment of AMPK2 activity with small-molecule inhibitors can be a useful strategy for the development of new medicines for stroke.

Despite the knowledge of the involvement of AMPK in various human diseases including type 2 diabetes, obesity, cancer, and stroke, the discovery of small-molecule inhibitors has lagged behind the neurobiological and pharmacological studies. Only a few AMPK inhibitors have been reported so far including the BML-275 (compound **C**).[6] In recent years, three-dimensional (3D) structures of AMPK2 have been reported both in the resting form and in complex with ligands.[7−9] The presence of structural information about the ligand-binding site and the interactions with small-molecule ligands can make it possible to design the new potent AMPK2 inhibitors that may develop into drug candidates.

In this study, we aim to identify the new potent AMPK2 inhibitors through the structure-based drug design protocol that involves virtual screening of a chemical library with docking simulations and *in vitro* enzyme assay. Among the various subunits of AMPK, α2 is selected as the target protein because we focus our interest in the discovery of drug candidates for ischemic stroke. Virtual screening using molecular docking has not always been useful due to the imperfections of the scoring functions to estimate the binding affinity between the target protein and a putative ligand.[10,11] Prior to carrying out the virtual screening, therefore, we improve the existing scoring functions by the implementation of an accurate solvation model to reflect the effect of desolvation cost for a ligand on the binding affinity with respect to the target protein. This modification seems to prevent the binding affinity of a ligand with many polar groups from being overestimated in virtual screening,[12] which would have an effect of increasing the hit rate in the subsequent enzyme assays. To further enhance the possibility of finding the actual inhibitors in virtual screening,

**Received:** April 8, 2014
**Published:** June 10, 2014

we apply the consensus scoring method with which one can take the advantages and supplement the deficiencies of various scoring functions.[13] The merit of this consensus scoring has been well appreciated in the discovery of the novel inhibitors of various target proteins.[14−16] It is thus expected for the present virtual screening procedure to be useful for enriching the chemical library with molecules that have good inhibitory activity against AMPK2.

## COMPUTATIONAL AND EXPERIMENTAL METHODS

**Preparation of Atomic Coordinates of AMPK2 and The Chemical Library.** 3D atomic coordinates of AMPK2 were prepared from its X-ray crystal structure in complex with compound **C** (PDB code: 3AQV)[9] as the receptor model for the structure-based virtual screening to identify the new potent inhibitors from a large chemical database. Special attention was paid to the determination of the protonation states for the ionizable residues of AMPK2. For example, we assumed that the side chains of Asp and Glu residues were neutral if either of their carboxylate oxygens was directed toward a hydrogen bond-accepting group such as the backbone aminocarbonyl oxygen within the distance of 3.5 Å, which is a generally accepted distance limit for the hydrogen bond of moderate strength.[17] Similarly, the side chains of lysine residues were assumed to be protonated unless the NZ atom stayed in proximity to a hydrogen bond-donating group. The same procedure was also applied for determining the protonation states of His residues. After the addition of all hydrogen atoms, we carried out 200 cycles of energy minimization for AMPK2 in complex with compound **C** to remove the bad steric contacts.

The docking library for AMPK2 was constructed from the commercial chemical database distributed by Interbioscreen (http://www.ibscreen.com) containing approximately 500,000 synthetic and natural compounds. At first, all these molecules were filtrated according to Lipinski's "Rule of Five" to select only the ones with the physicochemical properties of potential drug candidates[14] and without reactive functional group(s). To remove the redundancy in the chemical library, the structurally similar molecules with Tanimoto coefficient larger than 0.8 were clustered into a single representative one. As a consequence of the two-step filtering procedure, a docking library consisting of about 260,000 compounds was constructed. To obtain the 3D atomic coordinates of all molecules in the docking library, we used the CORINA program with which a stable molecular conformation could be generated using the conformational parameters derived from the X-ray crystal structures of small molecules contained in the Cambridge Structural Database.[19] Finally, the atomic charges were assigned for all molecules in the docking library with Gasteiger−Marsilli method[20] to make it possible to compute the electrostatic interaction energies with respect to AMPK2 in docking simulations. To apply the consensus scoring method in the virtual screening of AMPK2 inhibitors, we used the AutoDock program of version 3.5[21] in combination with the FlexX program[22] implemented in SYBYL 6.9. Docking simulations with the two programs were carried out in the ATP-binding pocket of AMPK2 to score and rank the compounds in the docking library according to the estimated binding affinities.

**Scoring.** The scoring functions used in a variety of docking programs to calculate the binding affinity between the target protein and a putative inhibitor may be categorized into two types: force field-based and empirical scoring functions. The former can be represented by a potential energy function that sums over all atomic contributions to protein−ligand interactions including electrostatic, van der Waals, and hydrogen bond interactions. Empirical scoring functions are expressed as a sum of several parametrized functions and devised to reproduce the experimental data for binding free energies and binding modes. Although each scoring method was found to have some merits depending on the features of binding sites, the scoring functions that rely purely on force field-based or empirical method consistently have performed worse in docking simulations than those constructed by the combined methods.[23] To enhance the possibility of finding the actual inhibitors from virtual screening, we employed the consensus scoring approach to the discovery of new AMPK2 inhibitors using AutoDock and FlexX as the representative docking programs with the force field-based and empirical scoring functions, respectively.

The procedure of consensus scoring adopted in the present study is depicted in Figure 1. At first, docking simulations

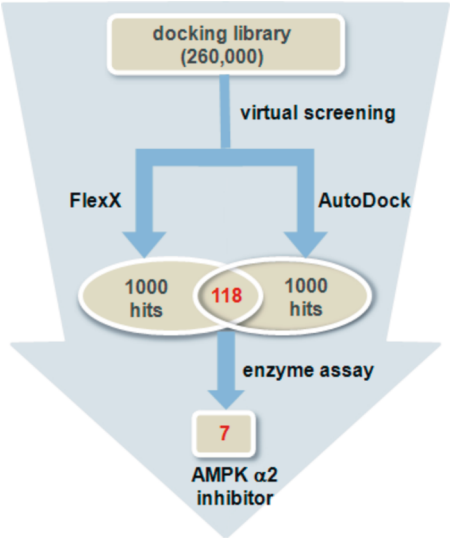


**Figure 1.** Flowchart for the discovery of AMPK2 inhibitors through the virtual screening with consensus scoring and enzyme assays.

between AMPK2 and the compounds in the docking library were carried out simultaneously with the AutoDock and FlexX programs to select 1000 top-scored compounds with each scoring function. The compounds included in both sets of virtual hits were then purchased from the compound supplier and tested for inhibitory activity against AMPK2 through the enzyme inhibition assays.

**Virtual Screening of AMPK2 Inhibitors with AutoDock.** The automated version of AutoDock program[24] was used to select the inhibitor candidates with force field-based scoring function. To improve the accuracy in docking simulations for virtual screening, we modified the original AutoDock scoring function to include the molecular solvation free energy term for organic molecules, which would have an effect of reflecting the contribution of the desolvation cost for a ligand to the protein−ligand binding affinity. This modified scoring function can be written as follows.

$$\Delta G_{\text{bind}}^{\text{aq}} = W_{\text{vdW}} \sum_{i=1} \sum_{j=1} \left( \frac{A_{ij}}{r_{ij}^{12}} - \frac{B_{ij}}{r_{ij}^{6}} \right) + W_{\text{hbond}} \sum_{i=1} \sum_{j=1} E(t) \left( \frac{C_{ij}}{r_{ij}^{12}} - \frac{D_{ij}}{r_{ij}^{10}} \right) + W_{\text{elec}} \sum_{i=1} \sum_{j=1} \frac{q_i q_j}{\varepsilon(r_{ij}) r_{ij}} + W_{\text{tor}} N_{\text{tor}} + W_{\text{sol}} \sum_{i=1} S_i (O_i^{\max} - \sum_{j \neq i} V_j e^{-r_{ij}^2/2\sigma^2}) \quad (1)$$

Here $W_{\text{vdW}}$, $W_{\text{hbond}}$, $W_{\text{elec}}$, $W_{\text{tor}}$, and $W_{\text{sol}}$ are the weighting factors of van der Waals, hydrogen bond, electrostatic interactions, torsional term, and solvation free energy of a putative inhibitor, respectively. $r_{ij}$ represents the interatomic distance, and $A_{ij}$, $B_{ij}$, $C_{ij}$, and $D_{ij}$ are associated with the depths of the potential energy well and the equilibrium separations between the two atoms. The hydrogen bond term has an additional weighting factor, $E(t)$, to represent the angle-dependent directionality. With respect to the distance-dependent dielectric constant ($\varepsilon(r_{ij})$), a sigmoidal function proposed by Mehler et al.[25] was used for the calculation of the interatomic electrostatic interactions between AMPK2 and the putative inhibitors. In the entropic term, $N_{\text{tor}}$ denotes the number of rotatable bonds in the ligand. In the solvation free energy term, $S_i$ and $V_i$ are the solvation parameter and the fragmental volume of atom $i$,[26] respectively, while $O_i^{\max}$ stands for the maximum atomic occupancy. In the calculation of molecular solvation free energy term in eq 1, we used the atomic parameters developed by Choi et al. because they proved to be successful in predicting the solvation free energies of a variety of organic molecules.[27] This modification of the scoring function seems to increase the accuracy in virtual screening of AMPK2 inhibitors because the underestimation of ligand solvation often leads to the overestimation of the binding affinity of an inhibitor with many polar atoms.[12] Indeed, the superiority of the modified scoring function to the previous one was well-appreciated in virtual screening of kinase and phosphatase inhibitors.[28,29]

**Virtual Screening of AMPK2 Inhibitors with FlexX.** All default parameters implemented in the Sybyl 6.9 program were used for docking simulations between AMPK2 and the compounds in the docking library. We defined the interaction surface in the ATP-binding pocket of AMPK2 with the cutoff distance of 6.5 Å and the reference ligand (compound **C**) whose binding mode had been determined by X-ray crystallographic analysis.[9] The conformational flexibility of a ligand was represented by a discrete set of preferred torsional angles with respect to acyclic single bonds. Base fragments were then selected automatically with the maximum number of 4. We placed a base fragment into the ATP-binding pocket based on the two algorithms. The first one overlay triples of interaction centers of the base fragment with triples of compatible interaction sites. When the base fragment had fewer than three interaction centers, we used the matching algorithm to find a suitable binding position in the ATP-binding pocket. To estimate the binding affinity of each candidate inhibitor, we combined the original empirical scoring function[30] with the solvation free energy term to reflect the effect of ligand solvation on protein−ligand docking. This modified scoring function can be expressed in the following form.

$$\Delta G_{\text{bind}}^{\text{aq}} = \Delta G_0 + W_{\text{hbond}} \sum_{\text{hbond}} f(\Delta R, \Delta\alpha) + W_{\text{ionic}} \sum_{\text{ionic}} f(\Delta R, \Delta\alpha) + W_{\text{aro/aro}} \sum_{\text{aro/aro}} f(\Delta R, \Delta\alpha) + W_{\text{lipo}} \sum_{\text{lipo}} f^*(\Delta R) + W_{\text{tor}} N_{\text{tor}} + W_{\text{sol}} \sum_{i=1} S_i (O_i^{\max} - \sum_{j \neq i} V_j e^{-r_{ij}^2/2\sigma^2}) \quad (2)$$

Here $\Delta G^0$ is a fixed ground term with the energy value of 1.29 kcal/mol. $f(\Delta R,\Delta\alpha)$ is a scaling function to penalize the deviations from the ideal distances and angles while $f^*(\Delta R)$ penalizes the forbiddingly close contacts in the lipophilic interactions involving the nonaromatic groups. With respect to the desolvation term, we adopted the same molecular solvation free energy function used in eq 1.

**Enzyme Inhibition Assay.** The inhibitory activities of the compounds selected in virtual screening against AMPK2 were measured using the CycLex AMPK2 Kinase Assay Kit (CycLex, Japan), which included the purified recombinant AMPK2 active in the form of $\alpha2/\beta1/\gamma1$ complex. All experiments for the measurement of AMPK2 enzyme activity assay were carried out according to the protocols provided by the manufacturer. At first, we activated the recombinant AMPK2 enzyme by the addition of a BSA-containing dilution buffer comprising 20 mM Hepes-KOH (pH 7.5), 10% BSA, 1 mM EDTA, 2 mM DTT, 50 mM NaCl, and 50% glycerol. ATP (50 $\mu$M) was also contained in this kinase reaction buffer to which 3 ng of active recombinant AMPK2 and the putative inhibitors were added. This reaction mixture was incubated with AMPK2 substrate (IRS-1 S789) precoated on 96 well plate at 30 °C for 30 min. Antiphospho-mouse IRS-1 S789 monoclonal antibody and HRP conjugated antimouse IgG were also incubated at room temperature for 30 min. Finally, the substrate reagent and the stop solution supplied by the manufacturer were added into 96 well. To measure the amount of AMPK activity, color development was recorded at the wavelength of 450 nm on the plate reader. Compound **C** was used as the positive control for the enzyme inhibition assay. We measured the inhibitory activities of the newly found AMPK2 inhibitors in duplicate at the concentrations of 0.0, 0.1, 0.3, 1, 3, 10, and 30 $\mu$M to obtain the dose−response curve fits. The $IC_{50}$ value of each inhibitor was then determined from direct regression analysis using the four-parameter sigmoidal curve as implemented in the SigmaPlot program.

## RESULTS AND DISCUSSION

As a check on the suitability of AutoDock and FlexX programs in virtual screening of AMPK2 inhibitors, we carried out docking simulations between AMPK2 and its known inhibitors for which the binding modes had been determined with X-ray crystallographic analysis. The X-ray structures of AMPK2 in complex with compound **C**[9] and staurosporin[31] were used in this validation study to assess the capability of AutoDock and FlexX scoring functions to reproduce the experimentally determined binding modes. As shown in Figure 2, the binding poses of compound **C** calculated from the two docking programs compare reasonably well with that in the original X-ray crystal structure with the associated root-mean-square deviation (RMSD) values of 0.89 and 1.43 Å for AutoDock and FlexX, respectively. In case of staurosporin, the RMSD values fall into 0.5 Å for both docking programs. These similarities between the calculated and experimental binding modes indicate the usefulness of AutoDock and FlexX scoring functions in virtual screening of AMPK2 inhibitors.

Of the 260,000 compounds screened for the possibility of tight binding in the ATP-binding pocket of AMPK2 with the modified AutoDock and FlexX scoring functions, a total of 118 compounds were included in both sets of 1000 top-ranked virtual hits. All these compounds selected from consensus scoring were purchased from the compound supplier and tested for the inhibitory activity against AMPK2. As a result, we found


dx.doi.org/10.1021/ci500214e | J. Chem. Inf. Model. 2014, 54, 2139−2146

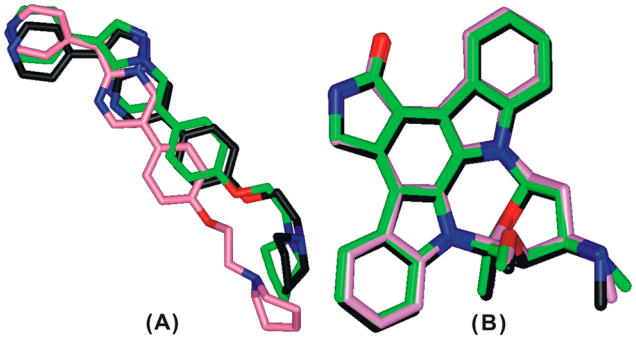


**Figure 2.** Structural alignment of the calculated binding modes of (A) compound **C** and (B) staurosporin with respect to those in the X-ray crystal structures. Carbon atoms of X-ray structure, AutoDock, and FlexX poses are indicated in black, green, and pink, respectively.

seven compounds that inhibited the kinase activity of AMPK2 by more than 50% at the concentration of 10 $\mu$M, which were selected to measure the $IC_{50}$ values. The chemical structures of the newly found inhibitors and their inhibitory activities are presented in Figure 3 and Table 1, respectively, together with those of the reference compound (compound **C**). Actually, none of these seven molecules has been reported as AMPK inhibitor neither in the literature and nor in the patent. Compounds **1**−**7** exhibit micromolar inhibitory activities against AMPK2 and possess multiple polar groups and nonpolar aromatic groups. Therefore, they seem to be stabilized in the ATP-binding pocket of AMPK2 through the multiple hydrogen bonds and hydrophobic interactions.

To compare the predicted binding modes with the AutoDock and FlexX scoring functions, we calculated the RMSD values between the most stable binding conformations of **1**−**7** obtained with the two docking programs. As shown in Table 1, the RMSD values fall into 1.2 Å for **1**−**3**, **5**, and **7**. This overall similarity in the binding poses calculated with the AutoDock and FlexX scoring functions can be understood in the sense that they comprise the energy terms with the same physical origins although the functional forms are different.

**Table 1. Inhibitory Activities of 1-7 and Compound C with Respect to AMPK2 and Their Rankings in Virtual Screening**

| compound | AutoDock ranking | FlexX ranking | RMSD (Å) | % inhibition at 10 $\mu$M | $IC_{50}$ ($\mu$M) |
|---|---|---|---|---|---|
| **1** | 6 | 22 | 0.83 | 1.1 | 1.4 |
| **2** | 56 | 291 | 0.46 | 17.4 | 2.7 |
| **3** | 224 | 450 | 0.91 | 19.4 | 3.0 |
| **4** | 102 | 71 | 2.59 | 20.7 | 4.6 |
| **5** | 637 | 524 | 1.15 | 21.4 | 5.5 |
| **6** | 318 | 806 | 2.70 | 39.0 | 6.3 |
| **7** | 716 | 121 | 1.02 | 42.4 | 8.1 |
| **C** | 492 | 1368 | 1.16 | 25.7 | 5.4 |

However, the difference between the two calculated binding modes increases significantly in **4** and **6** with the associated RMSD values larger than 2.5 Å. This may be attributed to the increase in the conformational degrees of freedom with the increase in molecular size, which would have an effect of making it difficult to sustain the consistency in docking results.

Also listed in Table 1 are the rankings of **1**−**7** and compound **C** in the virtual screening with the modified AutoDock and FlexX scoring functions. The AutoDock scoring function seems to perform a little better than the FlexX one because the rankings of the real inhibitors determined by the former are roughly higher than those based on the latter. However, we note that the rankings of **1**−**7** determined with the two scoring functions are independent each other; the squared Pearson correlation coefficient amounts to only 0.07, which indicates almost no correlation between the two results. This is actually not surprising for the large difference in the methods for calculating the binding free energy between the two scoring functions (eqs 1 and 2). It is also noteworthy that only three (**1**, **2**, and **4**) and two (**1** and **4**) inhibitors can be found if 118 candidates were selected according to the single scoring function of the AutoDock or FlexX program, respectively. This indicates that both scoring functions in themselves have limitation in terms of the accuracy and general applications. However, the probability of finding a good AMPK2 inhibitor

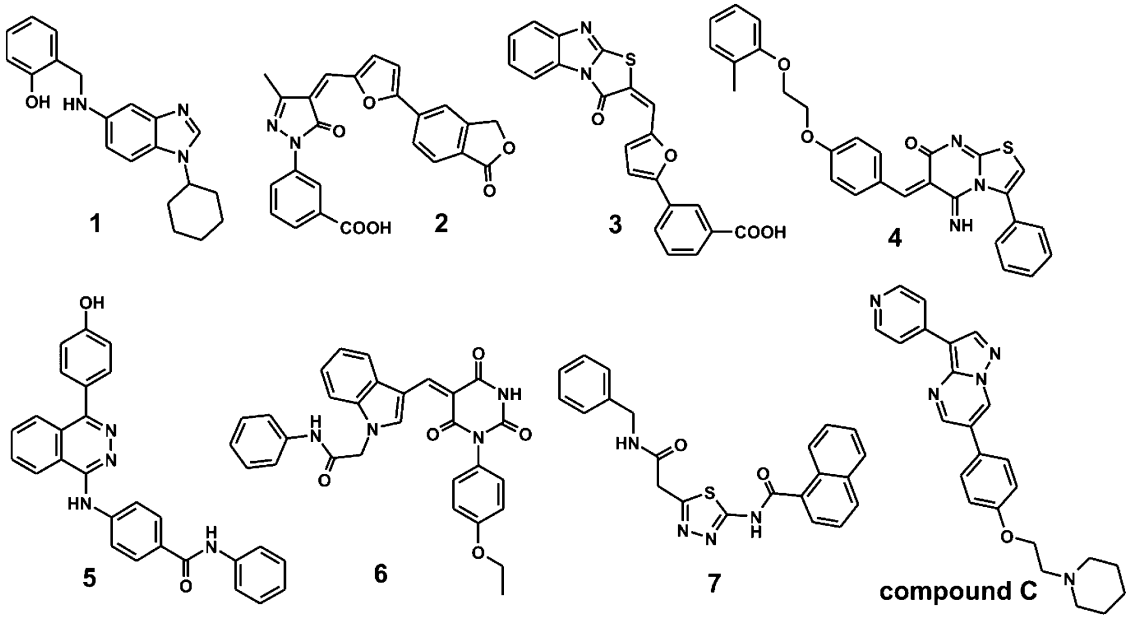


**Figure 3.** Chemical structures of compound **C** and seven AMPK2 inhibitors identified with the structure-based virtual screening.


dx.doi.org/10.1021/ci500214e | J. Chem. Inf. Model. 2014, 54, 2139−2146

with micromolar activity goes up to 5.9% if the candidate inhibitors were selected from the common virtual hits. The success rate in virtual screening of AMPK2 inhibitors can thus be enhanced substantially by applying the consensus scoring approach that makes it possible to take the advantages and balance the deficiencies of the force field-based and empirical scoring functions.

To examine the effects of ligand solvation on the binding affinity for AMPK2, we performed the decomposition analysis of the binding free energies of **1**−**7** calculated with the modified AutoDock and FlexX scoring functions. Because the free energy of binding for an enzyme−inhibitor complex in solution ($\Delta G^{aq}$) can be approximated as the difference between that in the gas phase ($\Delta G^{gas}$) and the solvation free energy of the inhibitor ($\Delta G^{sol}$),[12] we calculated the two energy terms separately to examine their relative contributions to $\Delta G^{aq}$. Table 2 lists the $\Delta G^{aq}$ values for the seven inhibitors calculated with the modified AutoDock and FlexX scoring functions together with their corresponding $\Delta G^{gas}$ and $\Delta G^{sol}$ values. The calculated binding free energies of **1**−**7** appear to become in better agreement with their experimental results for inhibitory activity as the original scoring functions lacking the ligand solvation term ($\Delta G^{gas}$) are improved by the addition of desolvation term ($-\Delta G^{sol}$) to form a physically more reasonable scoring function ($\Delta G^{aq}$). For example, the highest $\Delta G^{gas}$ values are obtained for **1** with the original AutoDock and FlexX scoring functions, which is inconsistent with its highest inhibitory activity against AMPK2 (Table 1) because the highest $\Delta G^{gas}$ values indicate the weakest interactions with AMPK2 among the seven inhibitors. On the other hand, $\Delta G^{sol}$ value of **1** appears to be higher than **2**−**7** by more than 5.4 kcal/mol, which indicates a substantial decrease in desolvation cost ($-\Delta G^{sol}$) for the former as compared to the latter. Compound **1** can thus be predicted to be the most potent AMPK2 inhibitor through the scoring with the $\Delta G^{aq}$ values that can reflect not only the increase in strengthening of the interactions with AMPK2 but also the decrease in desolvation cost for the formation of the required enzyme−inhibitor complex. This result exemplifies the necessity for the molecular solvation free energy term in the scoring functions. Such a large contribution of $\Delta G^{sol}$ to $\Delta G^{aq}$ also indicates that in order to enhance the potency of an inhibitor with structural changes, the resulting increase in the strength of enzyme−inhibitor interaction should be sufficient to surmount the increased stabilization of the inhibitor in aqueous solution.

**Table 2. Free Energy of Binding in the Gas Phase ($\Delta G^{gas}$) and in Aqueous Solution ($\Delta G^{aq}$) Calculated with AutoDock and FlexX Programs and Solvation Free Energy ($\Delta G^{sol}$) for the Seven AMPK2 Inhibitors**[a]

| compound | $\Delta G^{gas}_{AutoDock}$ | $\Delta G^{gas}_{FlexX}$ | $\Delta G^{sol}$ | $\Delta G^{aq}_{AutoDock}$ | $\Delta G^{aq}_{FlexX}$ |
|---|---|---|---|---|---|
| **1** | −24.12 | −22.24 | −12.63 | −11.49 | −9.61 |
| **2** | −28.58 | −25.07 | −18.12 | −10.46 | −6.95 |
| **3** | −26.89 | −23.78 | −18.06 | −8.83 | −5.72 |
| **4** | −29.70 | −28.45 | −20.08 | −9.62 | −8.37 |
| **5** | −28.48 | −26.59 | −21.26 | −7.22 | −5.33 |
| **6** | −28.78 | −24.43 | −20.59 | −8.19 | −3.84 |
| **7** | −25.13 | −26.32 | −18.46 | −6.67 | −7.86 |

[a]All $\Delta G$ values are given in kcal/mol and were calculated using the best binding conformations obtained from docking simulations.

The importance of $\Delta G^{sol}$ contribution to the scoring function can become more apparent when the calculated binding and solvation free energy values of **2** are compared with those of **1**. Although $\Delta G^{gas}$ values of **2** are predicted to be 4.5 and 2.8 kcal/mol lower than those of **1** by AutoDock and FlexX scoring functions, respectively, the 5.5 kcal/mol increase in desolvation cost for the inhibitor makes the $\Delta G^{aq}$ value of the former higher than that of the latter, which is consistent with the lower inhibitory activity of **2** than **1** (Table 1). On the other hand, **4**−**6** are included in the hits of virtual screening despite the high desolvation costs because they can bind tightly in the ATP-binding site, which is reflected in the highly negative $\Delta G^{gas}$ values. This indicates that the potency of an AMPK2 inhibitor can be augmented with structural modifications if the interaction between the new inhibitor and AMPK2 is made strong enough to overcome the increased stabilization of the inhibitor in aqueous solution. Judging from the intermediate $\Delta G^{gas}$ and $\Delta G^{sol}$ values, the inhibitory activities of **3** and **7** can be attributed to the combined effects of the binding in the ATP-binding pocket in moderate strength and the medium requirement for the desolvation cost. Thus, the decomposition analysis of $\Delta G^{aq}$ can also provide thermodynamic insight into the inhibition mechanism for the identified inhibitors because its sign and magnitude are determined by the combination of the strength of enzyme−inhibitor interaction ($\Delta G^{gas}$) and the desolvation cost for the inhibitor ($-\Delta G^{sol}$).

The importance of ligand solvation effects on the accuracy of virtual screening can be further assessed by comparing the calculated binding free energies and the experimentally determined $IC_{50}$ values of the seven inhibitors. For example, the squared Pearson correlation coefficient between the calculated binding free energies and experimental $IC_{50}$ values of **1**−**7** increases from 0.16 to 0.90 when the average value of $\Delta G^{gas}_{AutoDock}$ and $\Delta G^{gas}_{FlexX}$ is changed to that of $\Delta G^{aq}_{AutoDock}$ and $\Delta G^{aq}_{FlexX}$. This implies that the scoring function used in docking simulations may make sense only when the ligand solvation effects are taken into account.

To gain some structural insight into the inhibitory mechanisms of the identified AMPK2 inhibitors, we investigated their binding modes in the comparative fashion. The modified AutoDock scoring function was used in these binding mode analyses because it exhibited better performance than that of FlexX in the virtual screening. Overlaid in Figure 4 are the calculated lowest-energy conformations of **1**−**7** in the ATP binding pocket of AMPK2. All seven inhibitors appear to be accommodated in a unique binding pocket comprising N-lobe, C-lobe, and the hinge region of the ATP-binding site. The calculated binding modes of **1**−**7** are similar to that in the X-ray crystal structure of AMPK2 in complex with compound **C** in that they form several hydrogen bonds and van der Waals interactions with Ala43 and Lys45 in the N lobe, Tyr95 and Val96 in the hinge region, and Leu146, Ala156, and Met164 in the C lobe. It is also a common feature in the binding modes of **1**−**7** that some hydrophobic groups point toward the Gly loop that serves as the receptor for the phosphate group in ATP binding. Therefore, such an establishment of van der Waals contact with the Gly loop residues may contribute to the inhibition of AMPK2 by blocking the binding of ATP. To examine the possibility of the allosteric inhibition of AMPK2, we performed the additional docking simulations of **1**−**7** using the 3D grid maps constructed for its whole kinase domain. However, no peripheral binding pocket was found in these extended docking simulations for the newly identified

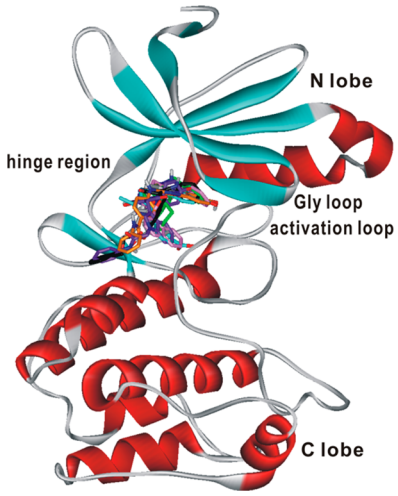


**Figure 4.** Calculated the binding modes of **1**−**7** in the ATP-binding pocket of AMPK2. Carbon atoms of **1**−**7** are shown in green, cyan, gray, black, orange, violet, and pink, respectively.

inhibitors. This supports the possibility that **1**−**7** would impair the activity of AMPK2 by specific binding to the ATP binding pocket.

We now turn to the identification of the detailed interactions relevant to the stabilization of the newly identified AMPK2 inhibitors in the ATP-binding pocket. The binding mode of **1** predicted by docking simulations with the modified AutoDock scoring function is shown in Figure 5. We note that the

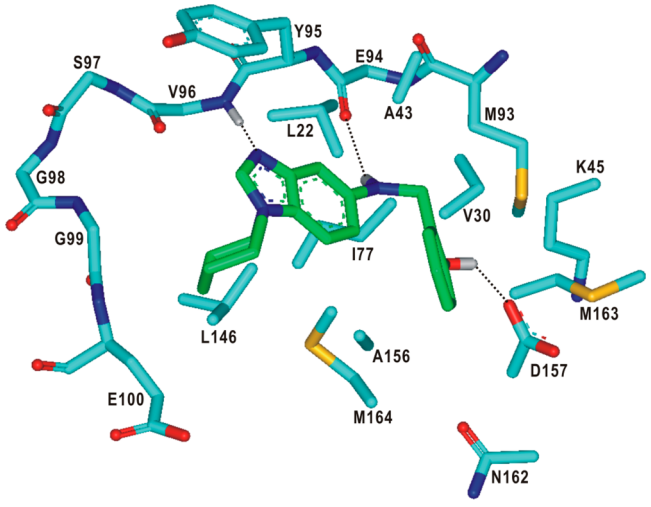


**Figure 5.** Binding configurations in the calculated AMPK2-**1** complex. Carbon atoms of the ligand and the protein are indicated in green and cyan, respectively. All dotted lines indicate a hydrogen bond.

benzoimidazole and the neighboring anilinic groups of **1** receive and donate a hydrogen bond from the backbone amidic nitrogen of Val96 and to the backbone aminocarbonyl oxygen of Glu94, respectively. These bidentate hydrogen bonds seem to be necessary for the inhibitory activity of **1** because the hydrogen bond interactions with backbone groups of the hinge region were found to play the role of anchoring compound **C** in the ATP-binding pocket of AMPK2.[9] In the calculated AMPK2-**1** complex, an additional hydrogen bond is established between the phenolic group of **1** and the side-chain carboxylate ion of Asp157. This hydrogen bond seems to be also one of the significant binding forces to stabilize **1** in the ATP-binding pocket because no stronger interaction involving an ionized group was observed in the AMPK2-**1** complex. The inhibitor **1** appears to be stabilized further in the ATP-binding pocket of AMPK2 through the establishment of the hydrophobic interactions between its nonpolar groups with the side chains of Leu22, Val30, Ala43, Ile77, Met93, Tyr95, Leu146, Ala156, Met163, and Met164. Judging from the pattern for the formation of AMPK2-**1** complex derived from docking simulations, the micromolar inhibitory activity of **1** can be attributed to the multiple hydrogen bonds and the hydrophobic interactions established simultaneously in the ATP-binding pocket.

Because **1** is relatively small in molecular size with the molecular weight of ∼320, it is anticipated to serve as a good starting point from which a variety of derivatives with high inhibitory activity can be obtained by chemical modifications. With respect to the design of the derivatives of **1** with increased inhibitory activity, the introduction of a small nonpolar group at the terminal phenol moiety seems to be a good choice because it resides in proximity to the small hydrophobic pocket comprising the side chains of Val30, Ala43, Ile77, Met93, and Met164 in the calculated AMPK2-**1** complex. It would also have an effect of enhancing the inhibitory activity of **1** to introduce a polar group at the terminal cyclohexyl group through the formation of hydrogen bonds with the backbone amide groups of Gly99 and Glu100.

Figure 6 shows the binding mode of **2** in the ATP-binding pocket of AMPK2 calculated with the modified AutoDock

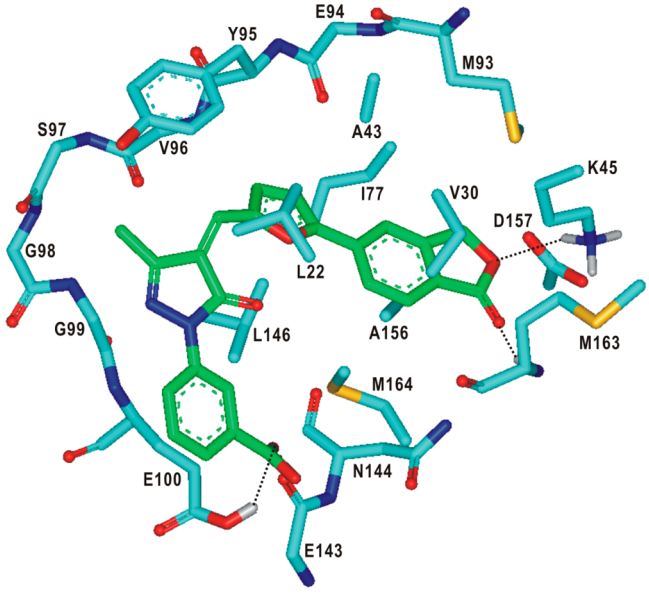


**Figure 6.** Calculated binding mode of **2** in the ATP-binding pocket of AMPK2. Carbon atoms of the ligand and the protein are indicated in green and cyan, respectively. All dotted lines indicate a hydrogen bond.

scoring function. It is shown that the terminal lactone group of **2** receives two hydrogen bonds from the side-chain ammonium ion of Lys45 and backbone amidic nitrogen of Met163 at the interface between the Gly loop and C lobe (Figure 4). A stronger hydrogen bond is established between the carboxylate ion of **2** and the side-chain carboxylic acid moiety of Glu100, which was assumed to be neutral because it had been found to play the role of hydrogen bond donor with respect to the


dx.doi.org/10.1021/ci500214e | J. Chem. Inf. Model. 2014, 54, 2139−2146

backbone aminocarbonyl oxygen of Glu143 in the X-ray crystal structure.[9] The pattern for the formation of hydrogen bonds in the AMPK2-**2** complex is quite different from that in the AMPK2-**1** complex in that the backbone groups of the hinge region are excluded in the former. However, the hydrogen boned interactions in the AMPK2-**2** complex seem to be stronger than those in the AMPK2-**1** complex because two charged groups are involved in the former as compared to only one in the latter. Consistent with the larger molecular size of **2** than **1**, van der Waals interactions in the AMPK2-**2** complex are established also in the stronger form that those in the AMPK2-**1** complex; nonpolar groups of **2** reside in close proximity to the side chains of Leu22, Val30, Ala43, Ile77, Met93, Tyr95, Leu146, Ala156, Met163, and Met164. Such a strengthening of the hydrogen bond and hydrophobic interactions may be invoked to explain the decrease in the $\Delta G^{gas}$ value by 3.6 kcal/mol on average in going from **1** to **2** (Table 2). Despite the strengthening of intermolecular interactions in the AMPK2-**2** complex, however, the inhibitory activity of **2** should be limited lower than that of **1** due to ~5.5 kcal/mol increase in desolvation cost for the inhibitor. Judging from the binding mode in the calculated AMPK2-**2** complex, the substitution of a small nonpolar group on the terminal isobenzofuran-1-one ring of **2** is likely to enhance the inhibitory activity due to the strengthening of hydrophobic interactions with the side chains of the residues in the Gly loop including Leu22, Val30, and Ala43.

As can be inferred from the overlaid docking poses in Figure 4, **3**-**7** exhibit a binding mode similar to that of **1** or **2** in that they are stabilized through the interactions with the residues in the hinge region and the interface of the N and C lobes. It is also a common feature in the calculated binding modes of **3**−**7** that they can form only one or no hydrogen bond with the backbone groups of the hinge region. Therefore, the chemical modifications to improve the inhibitory activities of **3**−**7** should be made in such a way to induce the new hydrogen bond interactions with the backbone amide groups in the hinge region.

Because the consensus scoring approach with the modified scoring functions of AutoDock and FlexX showed a good performance in virtual screening of AMPK2 inhibitors, the same scoring method seems to be also useful for designing the new potent inhibitors using **1**−**7** as a starting point. This can be made possible by carrying out the structure-based *de novo* design in the two steps. The first step involves the generation of various derivatives of **1**−**7** based on the structures of the AMPK2-inhibitor complexes obtained from docking simulations. Second, these randomly generated derivatives can be scored and ranked according to the binding affinity for AMPK2 using consensus scoring with the energy functions shown in eqs 1 and 2. The top-ranked derivatives selected in this way may be prepared by commercial purchase or chemical synthesis for biochemical evaluation. Related studies will be performed in the future for the discovery of potent AMPK2 inhibitors with nanomolar activity.

## ■ CONCLUSIONS

We aimed to identify the potent inhibitors of AMPK2 by means of a computer-aided drug design procedure involving structure-based virtual screening with docking simulations and *in vitro* enzyme assays. The consensus scoring method was employed in the virtual screening using the two docking programs, AutoDock and FlexX, to take advantage of and supplement the deficiencies of force field-based and empirical scoring functions. To further enhance the success rate to find the actual inhibitors, a molecular solvation free energy term was augmented to each scoring function. As a consequence of the efforts to improve the accuracy in virtual screening, we have been able to find seven AMPK2 inhibitors with micromolar inhibitory activity. Detailed binding mode analysis of the newly identified inhibitors showed that their binding in the ATP-binding pocket of AMPK2 would be facilitated by the formation of multiple hydrogen bonds with the backbone groups of the hinge region and/or the side chains of the residues at the interface between C and N lobes. Simultaneously, van der Waals interactions with the nonpolar residues around the ATP-binding pocket were also found to be the significant binding force to stabilize the AMPK2-inhibitor complexes. The present study demonstrated the usefulness of consensus scoring in the structure-based virtual screening with the modified AutoDock and FlexX scoring functions including the molecular solvation free energy term.

## ■ AUTHOR INFORMATION

### Corresponding Authors

*Telephone: +82-2-3408-3766. Fax: +82-2-3408-3334. E-mail: hspark@sejong.ac.kr (H.P).

*Telephone: +82-2-3408-3648. Fax: +82-2-3408-3661. E-mail: yhkim@sejong.ac.kr (Y.-H.K.).

### Notes

The authors declare no competing financial interest.

## ■ ACKNOWLEDGMENTS

This work was supported by Basic Science Research Program (2011-0022858), Brain Research Program (NRF-2009-0081490), and Midcareer Researcher Program (NRF-2011-0016050) through the National Research Foundation of Korea (NRF) grant funded by the Ministry of Education, Science and Technology.

## ■ REFERENCES

(1) Hardie, D. G.; Ross, F. A.; Hawley, S. A. AMPK: A nutrient and energy sensor that maintains energy homeostasis. *Nat. Rev. Mol. Cell. Biol.* **2012**, *13*, 251−262.

(2) Ramamurthy, S.; Ronnett, G. AMP-activated protein kinase (AMPK) and energy-sensing in the brain. *Exp. Neurobiol.* **2012**, *21*, 52−60.

(3) Viollet, B.; Athea, Y.; Mounier, R.; Guigas, B.; Zarrinpashneh, E.; Horman, S.; Lantier, L.; Hebrard, S.; Devin-Leclerc, J.; Beauloye, C.; Foretz, M.; Andreelli, F.; Ventura-Clapier, R.; Bertrand, L. AMPK: Lessons from transgenic and knockout animals. *Front. Biosci.* **2009**, *14*, 19−44.

(4) Li, J.; Zeng, Z.; Viollet, B.; Ronnett, G. V.; McCullough, L. D. Neuroprotective effects of adenosine monophosphateactivated protein kinase inhibition and gene deletion in stroke. *Stroke* **2007**, *38*, 2992−2999.

(5) Li, J.; Benashski, S. E.; Siegel, C.; Liu, F.; McCullough, L. D. Adenosine monophosphate activated protein kinase inhibition is protective in both sexes after experimental stroke. *Neurosci. Lett.* **2010**, *482*, 62−65.

(6) Zhou, G.; Myers, R.; Li, Y.; Chen, Y.; Shen, X.; Fenyk-Melody, J.; Wu, M.; Ventre, J.; Doebber, T.; Fujii, N.; Musi, N.; Hirshman, M. F.; Goodyear, L. J.; M?ller, D. E. Role of AMP-activated protein kinase in mechanism of metformin action. *J. Clin. Invest.* **2001**, *108*, 1167−1174.

(7) Xiao, B.; Sanders, M. J.; Underwood, E.; Heath, R.; Mayer, F. V.; Carmena, D.; Jing, C.; Walker, P. A.; Eccleston, J. F.; Haire, L. F.; Saiu, P.; Howell, S. A.; Aasland, R.; Martin, S. R.; Carling, D.; Gamblin, S. J. Structure of mammalian AMPK and its regulation by ADP. *Nature* **2011**, *472*, 230−233.

(8) Littler, D. R.; Walker, J. R.; Davis, T.; Wybenga-Groot, L. E.; Finerty, P. J.; Newman, E.; Mackenzie, F.; Dhe-Paganon, S. A conserved mechanism of autoinhibition for the AMPK kinase domain: ATP-binding site and catalytic loop refolding as a means of regulation. *Acta Crystallogr.* **2010**, *F66*, 143−151.
(9) Handa, N.; Takagi, T.; Saijo, S.; Kishishita, S.; Takaya, D.; Toyama, M.; Terada, T.; Shirouzu, M.; Suzuki, A.; Lee, S.; Yamauchi, T.; Okada-Iwabu, M.; Iwabu, M.; Kadowaki, T.; Minokoshi, Y.; Yokoyama, S. Structural basis for compound C inhibition of the human AMP-activated protein kinase 2 subunit kinase domain. *Acta Crystallogr.* **2011**, *D67*, 480−487.
(10) Huang, S. Y.; Grinter, S. Z.; Zou, X. Scoring functions and their evaluation methods for protein-ligand docking: recent advances and future directions. *Phys. Chem. Chem. Phys.* **2010**, *12*, 12899−12908.
(11) Warren, G. L.; Andrews, C. W.; Capelli, A. M.; Clarke, B.; LaLonde, J.; Lambert, M. H.; Lindvall, M.; Nevins, N.; Semus, S. F.; Senger, S.; Tedesco, G.; Wall, I. D.; Woolven, J. M.; Peishoff, C. E.; Head, M. S. A critical assessment of docking programs and scoring functions. *J. Med. Chem.* **2006**, *49*, 5912−5931.
(12) Shoichet, B. K.; Leach, A. R.; Kuntz, I. D. Ligand solvation in molecular docking. *Proteins* **1999**, *34*, 4−16.
(13) Charifson, P. S.; Corkery, J. J.; Murcko, M. A.; Walters, W. P. Consensus scoring: A method for obtaining improved hit rates from docking databases of three-dimensional structures into proteins. *J. Med. Chem.* **1999**, *42*, 5100−5109.
(14) Liu, S.; Fu, R.; Zhou, L. H.; Chen, S. P. Application of consensus scoring and principal component analysis for virtual screening against β-secretase (BACE-1). *PLoS One* **2012**, *7*, e38086.
(15) Kukol, A. Consensus virtual screening approaches to predict protein ligands. *Eur. J. Med. Chem.* **2011**, *46*, 4661−4664.
(16) Marsden, P. M.; Puvanendrampillai, D.; Mitchell, J. B. O.; Glen, R. C. Predicting protein−ligand binding affinities: A low scoring game? *Org. Biomol. Chem.* **2004**, *2*, 3267−3273.
(17) Jeffrey, G. A. *An Introduction to Hydrogen Bonding*; Oxford University Press: Oxford, 1997.
(18) Lipinski, C. A.; Lombardo, F.; Dominy, B. W.; Feeney, P. J. Experimental and computational approaches to estimate solubility and permeability in drug discovery and development settings. *Adv. Drug Delivery Rev.* **1997**, *23*, 3−20.
(19) Gasteiger, J.; Rudolph, C.; Sadowski, J. Automatic generation of 3D-atomic coordinates for organic molecules. *Tetrahedron Comput. Methodol.* **1990**, *3*, 537−547.
(20) Gasteiger, J.; Marsili, M. Iterative partial equalization of orbital electronegativity − A rapid access to atomic charges. *Tetrahedron* **1980**, *36*, 3219−3228.
(21) Morris, G. M.; Goodsell, D. S.; Halliday, R. S.; Huey, R.; Hart, W. E.; Belew, R. K.; Olson, A. J. Automated docking using a Lamarckian genetic algorithm and an empirical binding free energy function. *J. Comput. Chem.* **1998**, *19*, 1639−1662.
(22) Rarey, M.; Kramer, B.; Lengauer, T.; Klebe, G. A fast flexible docking method using an incremental construction algorithm. *J. Mol. Biol.* **1996**, *261*, 470−489.
(23) Kitchen, D. B.; Decornez, H.; Furr, J. R.; Bajorath, J. Docking and scoring in virtual screening for drug discovery: Methods and applications. *Nat. Rev. Drug Discovery* **2004**, *3*, 935−949.
(24) Park, H.; Lee, J.; Lee, S. Critical assessment of the automated AutoDock as a new docking tool for virtual screening. *Proteins* **2006**, *65*, 549−554.
(25) Mehler, E. L.; Solmajer, T. Electrostatic effects in proteins: comparison of dielectric and charge models. *Protein Eng.* **1991**, *4*, 903−910.
(26) Stouten, P. F. W.; Frömmel, C.; Nakamura, H.; Sander, C. An effective solvation term based on atomic occupancies for use in protein simulations. *Mol. Simul.* **1993**, *10*, 97−120.
(27) Choi, H.; Kang, H.; Park, H. New solvation free energy function comprising intermolecular solvation and intramolecular self-solvation terms. *J. Cheminform.* **2013**, *5*, 8.
(28) Park, H.; Hong, S.; Kim, J.; Hong, S. Discovery of picomolar ABL kinase inhibitors equipotent for wild type and T315I mutant via structure-based de novo design. *J. Am. Chem. Soc.* **2013**, *135*, 8227−8237.
(29) Park, H.; Yu, K. R.; Ku, B.; Kim, B. Y.; Kim, S. J. Identification of novel PTPRQ phosphatase inhibitors based on the virtual screening with docking simulations. *Theor. Biol. Med. Model.* **2013**, *10*, 49.
(30) Böhm, H. J. The development of a simple empirical scoring function to estimate the binding constant for a protein-ligand complex of known three-dimensional structure. *J. Comput.-Aided Mol. Des.* **1994**, *8*, 243−256.
(31) Xiao, B.; Sanders, M. J.; Carmena, D.; Bright, N. J.; Haire, L. F.; Underwood, E.; Patel, B. R.; Heath, R. B.; Walker, P. A.; Hallen, S.; Giordanetto, F.; Martin, S. R.; Carling, D.; Gamblin, S. J. Structural basis of AMPK regulation by small molecule activators. *Nat. Commun.* **2013**, *4*, 3017.